

**BUCKLING CAPACITY OF COLD-FORMED STEEL
STRUCTURE COLUMN MEMBER WITH PERFORATION
SECTION IN AFFORDABLE HOUSE FRAMING SYSTEM**

ZAFIRA NUR EZZATI BT MUSTAFA

**SCHOOL OF CIVIL ENGINEERING
UNIVERSITI SAINS MALAYSIA
2017**

Blank Page

BUCKLING CAPACITY OF COLD FORMED STEEL STRUCTURE
COLUMN MEMBER WITH PERFORATION SECTION IN
AFFORDABLE HOUSE FRAMING SYSTEM

By

ZAFIRA NUR EZZATI BT MUSTAFA

This dissertation is submitted to

UNIVERSITI SAINS MALAYSIA

As partial fulfilment of requirement for the degree of

**BACHELOR OF ENGINEERING (HONS.)
(CIVIL ENGINEERING)**

School of Civil Engineering,
Universiti Sains Malaysia

June 2017



**SCHOOL OF CIVIL ENGINEERING
ACADEMIC SESSION 2016/2017**

**FINAL YEAR PROJECT EAA492/6
DISSERTATION ENDORSEMENT FORM**

Title: BUCKLING CAPACITY OF COLD-FORMED STEEL STRUCTURE
MEMBER WITH PERFORATION SECTION IN AFFORDABLE
HOUSE FRAMING SYSTEM

Name of Student: ZAFIRA NUR EZZATI BT MUSTAFA

I hereby declare that all corrections and comments made by the supervisor(s) and
examiner have been taken into consideration and rectified accordingly.

Signature:

Approved by:

(Signature of Supervisor)

Date :

Name of Supervisor :

Date :

Approved by:

(Signature of Examiner)

Name of Examiner :

Date :

ACKNOWLEDGEMENT

Firstly, I would like to thanks to Universiti Sains Malaysia for giving me this opportunity to complete my FYP dissertation. Throughout this one year, I would like to convey my appreciation and thankfulness to my supervisor Assoc. Prof. Dr. Fatimah De'nan for her guidance, support, suggestion and advices and constructive comment throughout the process of this study. She inspired me greatly to work in this research. Furthermore, my sincere and special thanks to Dr Mustafasanie M.Yussof for his guidance especially on finite element LUSAS software. Without them, I hardly get my result.

I would like to thank my friend Lee Kent Zhen who always support me and work together to produce a better quality dissertation. Very special thanks to my love, Homare-San, for always be number one supporter during my hard time finishing this project. All day and all night is all about my Finale Year Project. Thank for cheering me up.

Lastly, a very big thanks to my beautiful family member who always giving good words to me. Without them I could not finish my dissertation and even get my degree. Thank you very much to everyone.

ABSTRAK

Tetiang C terbentuk sejuk biasa digunakan dalam pembinaan dinding pasang siap. Disebabkan isu tentang kos keseluruhan keluli menjadi pertimbangan utama dalam rancangan membina rumah mampu milik untuk mangsa banjir, sector pembinaan memperkenalkan konsep bukaan pada bahagian web. Oleh itu, dalam kajian ini, kajian berangka menumpukan pada kapasiti kekuatan lengkokan dengan pembukaan pada web tetiang telah dijalankan. Ujikaji dimulakan dengan menentukan jarak antara tetiang yang sesuai untuk kerangka rumah. Analisis kerangka dilakukan menggunakan STAAD Pro. menggunakan tetiang C tanpa tembukaan. Pembukaan berbentuk bulat digunakan dalam ujikaji ini dengan saiz 0.4D, 0.6D, dan 0.8D ($D=180\text{mm}$). Jarak diantara pembukaan adalah 150mm, 250mm dan 350mm. Untuk specimen bukaan 0.4D dan jarak antara hujung tetiang dan pembukaan bulat adalah 539mm mempunyai capacity lengkukan yang paling tinggi (26.59 kN). Pengurangan kapasiti lengkukan adalah 5.31% daripada kapasiti lengkukan tetiang C tanpa pembukaan dan pengurangan isipadu adalah sebanyak -2.16%. untuk kes yang sama tetapi saiz bukaan 0.8D, ia mengurangkan kapasiti lengkukan sebanyak 22.52% dan isipadu -6.85%. Kesimpulannya, kajian ini telah menunjukkan tetiang C yang tidak mempunyai bukaan mempunyai keupayaan lengkukan yang lebih tinggi.

ABSTRACT

Cold formed C-column have been used in interior wall construction. Because of the issue of material cost become one of the factors need to be considered in affordable house construction, the construction sector has introduced the concept of opening to the column web. Besides, this study focus on the buckling capacity for C-column cold formed steel with perforation. This study starts with determining the suitable spacing for the space column for the affordable house. Analysis house frame has been done in STAAD Pro. analysis using C-column without perforation. Opening with circular shape has been used in this study with the size of 0.4D, 0.6D and 0.8D (D=180mm). Spacing within the opening is 150mm, 250mm and 350mm. for the specimen with 0.4D opening and the edge distance is 539mm have the highest buckling capacity (26.59 kN). Reduction of buckling capacity is 5.31% from C-column without perforation and reduction of volume is -2.16%. for the same case with 0.8D opening, the buckling capacity reduce with 22.52% and volume is -6.85%. the conclusion of this study, C-column without perforation have higher buckling capacity compare to C-column with perforations.

TABLE OF CONTENTS

ACKNOWLEDGEMENT	II
ABSTRAK	III
ABSTRACT	IV
TABLE OF CONTENTS	V
LIST OF FIGURES	VII
LIST OF TABLES	XI
LIST OF ABBREVIATIONS	XIII
NOMENCLATURES	XIV
CHAPTER 1	1
1.1 Introduction	1
1.2 Problem statement	3
1.3 Objective of study	4
1.4 Scope of study.....	4
CHAPTER 2	6
2.1 Introduction	6
2.2 Steel with Perforated Section.	6
2.3 Steel Section under buckling load.....	10
2.4 Cold-formed steel section.....	15
2.5 Summary	24
CHAPTER 3	25
3.1 Introduction	25
3.2 Steel Framing Design Using STAAD Pro.....	25
3.2.1 Modelling Procedure.....	30
3.3 Finite Element Analysis using LUSAS.....	36
3.3.1 Model Attributes	36
3.3.2 Modelling Procedure.....	40
3.4 Convergence Study	51
3.5 Terminology used for the section	53

3.6	Summary	53
CHAPTER 4.....		54
4.1	Introduction	54
4.2	Framing design in STAAD. Pro Analysis.....	54
4.2.1	Space column design with different spacing.	55
4.2.2	Final framing Design with bracing.....	58
4.2.3	Redesign Critical column from STAAD. Pro to LUSAS	60
4.3	LUSAS Analysis for cold-formed C-channel with and without perforation.....	64
4.3.1	Eigenvalue analysis for buckling behaviour study with different parameters... ..	64
4.4	Parametric study	76
4.4.1	Effect of perforation spacing.....	76
4.4.2	Effect of different edge distance on buckling.	79
4.4.3	Effect of different size of perforation together with edge distance	80
4.5	Volume Reduction Due to Presence of Opening	84
4.6	Data verification using LUSAS analysis with STAAD Pro. Analysis	87
4.7	Discussion.....	90
4.8	Summary	92
CHAPTER 5.....		93
5.1	Summary	93
5.2	Recommendation for further research.....	94
REFERENCES.....		95

LIST OF FIGURES

Figure 1.1: Typical Cold-formed Steel Framing (Green Building, 2016)	2
Figure 2.1: CUFSM approximate method for calculating P_{cr}	7
Figure 2.2: Vierendeel mechanism along a circular web opening (Tsavdaridis, 2012) ..	9
Figure 2.3: Axial stress distributions of non-perforated compression.....	10
Figure 2.4: The 7 Degree-of-freedom 2-node Beam Element (Mansur, 1992)	11
Figure 2.5: Critical buckling modes with FEA-ADAPTIC and EFG/RSA models	12
Figure 2.6: Load – Deflection plot for Case 1 FE models (Krishnarani,2016)	14
Figure 2.7: Load – Deflection plot for Case 2 FE models (Krishnarani,2016)	14
Figure 2.8: Load – Deflection plot for Case 3 FE models (Krishnarani,2016)	15
Figure 2.9: Test set up (Kalavagunta, 2013).....	16
Figure 2.10: Section dimension for C100 section (Kalavagunta, 2013).....	16
Figure 2.11 Graph Ultimate Load Experimental versus	18
Figure 2.12: MLC Beams (F.Portio,2012).....	19
Figure 2.13: Experimental Load Deflection curves of the MLC Beam (F.Portio,2012)	20
Figure 2.14: Comparison of (F- δ) curve for different connection spacing (F.Portio,2012)	21
Figure 2.15: CU-BEAM analysis (B.P. Gothuru et al., 2000).....	22
Figure 2.16: Test Rb- Rotation at midspan (B.P. Gothuru et al., 2000)	23
Figure 2.17: Test C12U – effect of warping fixity (B.P.Gothuru,1999)	23
Figure 3.1: Proses STAAD Pro. performing analysis.....	29
Figure 3.2: Generating new model.....	30
Figure 3.3: Parametric structure window	31
Figure 3.4: Coordinate input.....	31
Figure 3.5: Steel structure Frame.....	32

Figure 3.6: Properties section	33
Figure 3.7: Load case window	33
Figure 3.8: Running the analysis	34
Figure 3.9: Setting up result.....	35
Figure 3.10: Result from analysis	35
Figure 3.11: Procedure for Lusas analysis	39
Figure 3.12: ‘New model’ window	40
Figure 3.13: ‘Enter coordinate’ window	41
Figure 3.14: Creating line	41
Figure 3.15: ‘Copy’ window.....	42
Figure 3.16: C channel member.....	42
Figure 3.17: Location of ‘Coords/Point’	43
Figure 3.18: ‘Arc/Circle Definition’ window	43
Figure 3.19: Creation of circle	44
Figure 3.20: Creating hole	44
Figure 3.21: ‘Copy’ window for creating more holes.....	45
Figure 3.22: Complete perforation section	45
Figure 3.23: ‘Surface Mesh’ input.....	46
Figure 3.24: ‘Geometry Surface’	46
Figure 3.25: Support toolbar	48
Figure 3.26: Table for loading value.....	48
Figure 3.27: Mesh Element.....	49
Figure 3.28: Applying Load.....	49
Figure 3.29: Assigning eigenvalues	50
Figure 3.30: Set the eigenvalue.....	50

Figure 3.31: Analysis button.....	51
Figure 3.32: Graph of resultant displacement against number of elements.....	52
Figure 3.33: Typical column member with perforation.....	53
Figure 4.1: Space column with 300mm spacing.....	56
Figure 4.2: Space column with 500mm spacing.....	57
Figure 4.3: Space column with 1000mm spacing.....	58
Figure 4.4: Complete space column with 1000mm spacing.....	59
Figure 4.5: Complete space column with 1000mm spacing.....	59
Figure 4.6: The critical column with vertical loading in x-axis from STAAD Pro. analysis	61
Figure 4.7: Displacement of critical column from STADD Pro. Analysis.....	62
Figure 4.8: Non perforated column form STAAD Pro. into LUSUS analysis.....	63
Figure 4.9: Typical column section with perforations.....	65
Figure 4.10: Column with 0.4D opening.....	67
Figure 4.11: Column with 0.6D perforation.....	70
Figure 4.12: Column with 0.8D perforation.....	73
Figure 4.13: Typical column with perforation section.....	76
Figure 4.14: Buckling load versus spacing of perforation distance with 3 holes.....	78
Figure 4.15: Buckling load versus spacing of perforation distance with 5 holes.....	78
Figure 4.16: Buckling load versus Edge distance graph.....	80
Figure 4.17: Buckling load versus perforation size graph.....	82
Figure 4.18: Buckling load versus perforation size.....	83
Figure 4.19: Graph of Percentage different of buckling capacity versus.....	86
Figure 4.20: Maximum reaction in z-axis direction from roof truss analysis using LUSAS	88

Figure 4.21: Maximum reaction in z-axis direction from roof truss analysis using
STAAD Pro..... 89

LIST OF TABLES

Table 2.1: Parameters consideration for sinusoidal opening (Krishnarani,2016).....	13
Table 2.2: Axial Compression test result Experimental versus	17
Table 2.3: Axial Compression test result: Experimental versus	17
Table 2.4: Testing program (F.Portio,2012)	19
Table 3.1: Data of maximum nodal displacement of C-section Purlin model.....	52
Table 4.1: Summary for space column with 300mm spacing deflection.....	56
Table 4.2: Summary for space column with 500mm spacing deflection.....	57
Table 4.3: Summary for space column with 1000mm spacing deflection.....	58
Table 4.4: Summary for complete space column design with.....	60
Table 4.5: Buckling moment for different size of perforation 0.4D with opening spacing for 1.75m column.....	68
Table 4.6: Buckling moment for different size of perforation 0.6D with opening spacing for 1.75m column.....	71
Table 4.7: Buckling moment for different size of perforation 0.8D with opening spacing for 1.75m column.....	74
Table 4.8: Buckling load for different type of perforations spacing.....	77
Table 4.9: Buckling load for different type of edge distance with	80
Table 4.10: Buckling load for different size of perforation with.....	81
Table 4.13: Percentage Different of Volume Due to Opening Size 0.4D for 1.75m Column.....	85
Table 4.14: Percentage Different of Volume Due to Opening Size 0.6D for 1.75m Column.....	85
Table 4.15: Percentage Different of Volume Due to Opening Size 0.8D for 1.75m Column.....	86

Table 4.16: Table of comparison between LUSAS analysis and manual calculation ...	90
Table 4.17: Best selection of model after analysis	91

LIST OF ABBREVIATIONS

DM	Damage Measure
EC1	Eurocode 1
EC8	Eurocode 8
EDP	Engineering Demand Parameter
EN	European Standard
FE	Finite Element
CFS	Cold-Formed Steel
BS5950	British Standard 5950
MLC Beam	Modular Light-weight Cold-Formed Beam
AISI	American Iron and Steel Institute

NOMENCLATURES

$(F_b)_{ult}$	Ultimate base shear
F_i	Equivalent static force for each storey level
F_{ult}	Ultimate force
F_y	Yield force
M_{GQ}	Bending moment
M_L	Magnitude in Richter scale
M_T	Total moment capacity
M_w	Moment magnitude
D_o	Depth of opening
S	Sinusoidal opening
h_w	Corrugation Height
d_f	Rivet Spacing
f_o	Web Stiffeners
F_u	Ultimate Force
δ_u	Ultimate Deflection

CHAPTER 1

INTRODUCTION

1.1 Introduction

The new generation of steel has to give a lot of advantage to humankind. Harvesting new idea in construction industry always giving best solution for multitasking problem. Using cold formed steel giving a lot of advantages such as lightweight, excellent strength to weight ratio, easy to be instal, fast construction process and the availability of various shape of the structural steel element. In order to design the most efficient affordable housing, cold formed steel is one of the best choice to be used as structural element. Furthermore, the advantage of cold formed steel meet the criteria that been required for affordable house design. The popularity of cold-formed steel sections has effectively increased due to its advantages such as light weight, cost-effectiveness, fast and easy erection, high strength-to-weight ratio, mass production and recyclable when compared with hot rolled section. The building material encompasses columns, beams, joist, studs, floor decking, built-up sections and other components. The structure channel or C column were used primarily in building construction and civil engineering. Its cross section consists of a wide web and two flanges at the top and bottom of the web. C-channel have been used as purlin, beam and column. Cold formed C-channel are categorised based on their size and its strength. Creating an opening in the web of beam or column can give some advantage in the construction industry. Basically, having an opening web giving an advantage for mechanical and electrical services so the height of ceiling can be reduced. But reducing area of steel can cause reduction of the steel capacity to withstand the load. In order to provide an opening to the structure member, the designer

must know what the limit that needs to be taken into design consideration. The opening causes a reduction of buckling capacity of the web depend on certain factors such as the size of the opening, edge distance and opening spacing. In order to determine the best perforation section, an analysis needs to be done by using finite element. The cold formed section must have sufficient buckling capacity in order to resist the vertical loading. To determine the buckling capacity of the section, a series of eigenvalue will be perform from Finite Element analysis. From the eigenvalue, conclusion can be made to understand which parameters which influenced the buckling capacity of the section. Global buckling, also known as Euler buckling, defines buckling of the full member at long half-wavelengths including both flexural and flexural-torsional effects.



Figure 1.1: Typical Cold-formed Steel Framing (Green Building, 2016)

1.2 Problem statement

Nowadays, the flood has become one of the common natural disasters that happened in Malaysia. These phenomena cause a lot of destructions and most of the victims lost their house. Because of unpredictable event happened, government take an initiative to build an affordable house which is easy to be built, low cost and economical can be installed without big machinery and supervision from an engineer. The aim of this project is to produce an affordable design with the most efficient way in term of cost and construction method.

In order to design an affordable house using cold formed, a suitable structural design system need to be applied in such a way it can perform as a stable structure. In this study, space frame structural system including space column have been proposed. But, the house frame design needs a suitable space column by determining the most suitable column spacing. This study needs to be done because there is specific design specification that can be used as a design reference. The space column is made up from cold formed C-channel with perforation but until now there is no catalogue that shows the capacity for cold-formed steel with perforation section.

The capacity of cold-formed with perforation section depend on the perforation parameters. The important factor that influences the buckling capacity of the section the parameter of the perforation section. Thus the suitable of perforation size, spacing distance and the edge distance still become a question to the structural designer. The buckling capacity of perforation section must be adequate to the capacity that being required from the frame house design.

In this study, the parameter of the perforated section needs to be suitable in order to get the most optimum design. The perforated section must have sufficient distance and dimension for each

perforated section. Besides, through analysis is the best prediction for buckling capacity of the section with an opening. The buckling capacity of C-channel section with the opening needs to compare with C-channel section without opening in the selection process.

1.3 Objective of study

The objective of this study are:

1. To determine the most efficient cold formed steel framing system for the affordable house.
2. To determine buckling capacity for cold formed C-channel steel purlin with perforation.
3. To determine the most suitable C-column with perforation to be used for the affordable house.

1.4 Scope of study

The list of job scope in this study:

1. STAAD-PRO software is used to generate affordable house framing system using cold-formed C-channel (180 × 75 ×20) section.
2. Design the most efficient frame system with suitable spacing of space column.
3. Identify critical column from the steel frame analysis in STAAD Pro. then analyses the cold formed steel column with perforation section in LUSAS.

4. Assign same properties and same concentrated load in vertical direction to both the C-channel single purlin with and without openings.
5. The buckling behaviour of C-channel single purlin with various openings was studied.
6. Calculate the percentage of material cost saving compare to non-perforated cold formed steel.

CHAPTER 2

LITERATURE REVIEW

2.1 Introduction

In this project, the major concerns are to reduce the weight and cost of the component parts and to ensure the frame structure is saved. The lighter weight of material that is used in the frame system help to reduce the dead load of the structure. At the end of this study, the steel member will be modified with perforation section in order to reduce the volume of the steel member. Thus, reduction of steel volume makes the steel section become lighter.

2.2 Steel with Perforated Section.

The judicious placement of the hole in the C-channel section of cold-formed steel has been employed to design lighter and stiffer beams for over 100 years. D. Moen (2008) with the research of direct strength design cold-formed steel members with perforation. Cold-formed steel (CFS) structural member are commonly manufactured with holes to accommodate plumbing, electrical, and heating conduits in wall and ceilings of the building. The structural designer is available to predict the strength of CFS members with holes are prescriptive and limited to specific perforation location, spacing and sizes using current design method. The elastic buckling properties of the rectangular plate and cold-formed steel beams and columns, including the presence of holes, are studied with thin shell finite element Eigen buckling analysis. In this study, the buckled mode shapes unique to members with the hole are categorised.

With the presence of holes, P_{crd} assumes that the change in cross section stiffness within a distortion half-wave can be stimulated by assuming a reduced thickness of the cross section. First, the distortional half-wavelength of the cross-section, L_{crd} , without holes is determined. The elastic buckling curve is calculated using the gross section of the column in CUFSM and L_{crd} is read off of the curve at the location of the distortional local minimum as shown in Figure 2.1, the result shows that L_{crd} does not change with the presence of hole within the distortional half-wavelength. Then the cross section is modified to account for the presence of a hole. Another elastic buckling curve is generated and P_{crd} is determined as the elastic buckling load accruing at L_{crd} .

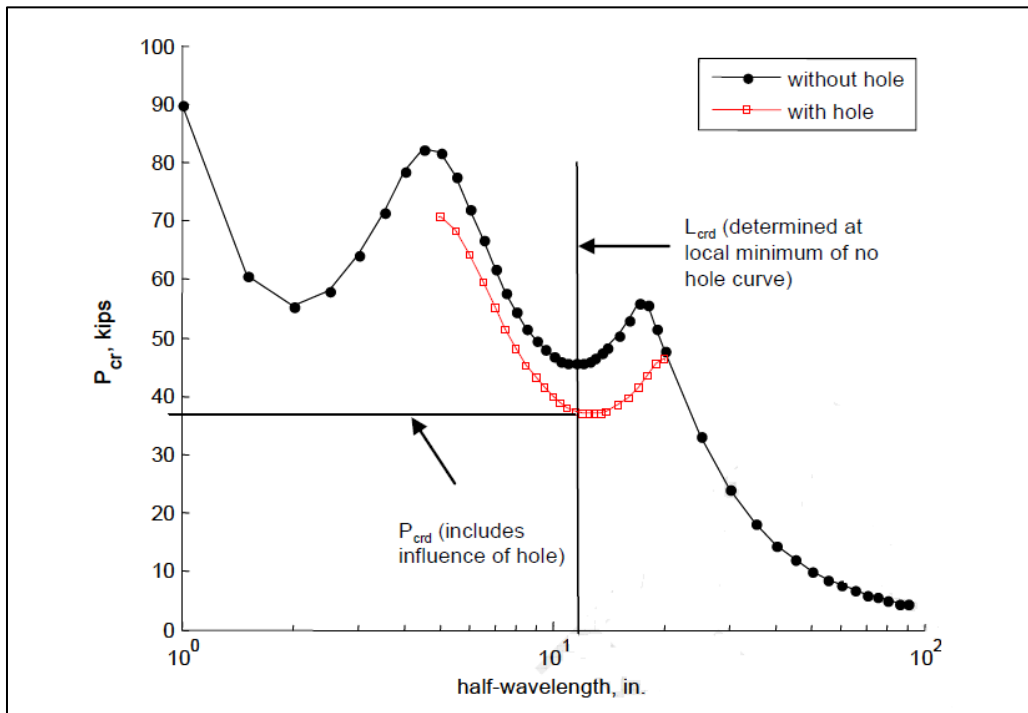


Figure 2.1: CUFSM approximate method for calculating P_{cr} for a column with holes (D. Moen, 2008)

Because of a thin and perforated section, the steel section can improve the weight-to-stiffness ratio. Introducing an opening in steel web giving ability to integrate building services into the structure depth and the perceived aesthetic appeal of the beam. When coming to hot rolled steel member, it buckling constitutes a failure. Compare to cold-formed steel member, it includes the post-local buckling strength. The post-buckling strength of cold-formed steel member could be larger than the actual buckling loads.

When perforation steel is subjected to loading, most findings relate to vierendeel failure. When high shear force acting on the beam, vierendeel act as a failure mechanism. The beam which associated with large web openings is the main factor it becomes a dominant failure (Tsavdaris et al., 2012). At the corner of opening shapes or at specific deform T-section above the web opening formed a plastic hinge. The local bending moment occurs when vertical shear force transfer across the web opening. This what researcher called vierendeel bending moment which is the main cause of vierendeel failure. Seo and Mahendran (2012) state that when continuous development of plastic hinge at the ends of four T-section above and below the opening, it causes vierendeel mechanism. This failure is a combination of vierendeel bending moment, local axial force and local shear force.

Chung et al. (2000) investigate the failure mechanism of the steel beam with a circular opening. Formation of the plastic hinge will be the limit state of loading capacity for the beam at the top T-section on the lower moment. Figure 2.2 shows critical location of the perforated section which vierendeel mechanism tend to form. The moment capacity of the T-sections above and below the web openings under co-existing axial and shear force was assessed by linear interaction formula. Usually, failure does not always occur at the bottom moment side and plastic hinge tends

to form at top T-section. Thus, current design method was examined in detail with plastic hinges formed on the lower moment side (LMS) and the high moment side (HMS) of the web opening separately.

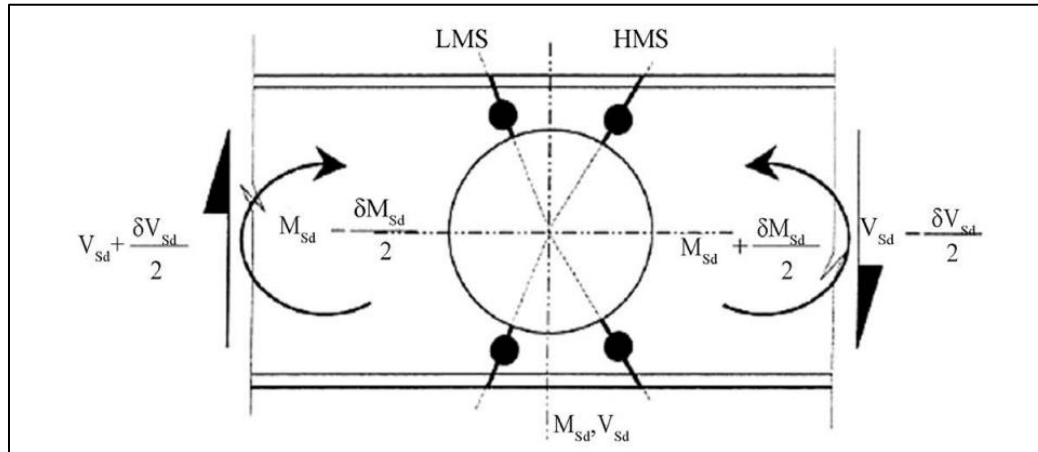


Figure 2.2: Vierendeel mechanism along a circular web opening (Tsavdaridis, 2012)

A. Rahman (1998) study about cold-formed steel compression members with perforations. A finite element study was performed on perforated lipped channel CFS member compression, using the finite element model development. In Figure 2.3, shows the result of the performance finite element study includes the behaviour of the axial stress distribution and the effective design width of the perforated web plate of the CFS compression member. The effective design width of the perforated plate was predict based on the finite element ultimate load results of the compression members. The axial compressive stress capacity and the prediction effective design width of the perforated web plate were found to decrease significantly with the increase of perforation width, the plate slenderness ration, and the yield strength of the material. One of the main observation of

Mahmoud's study was that a transfer axial stress occurs from the central part of the perforated compression plate to the side of the perforation.

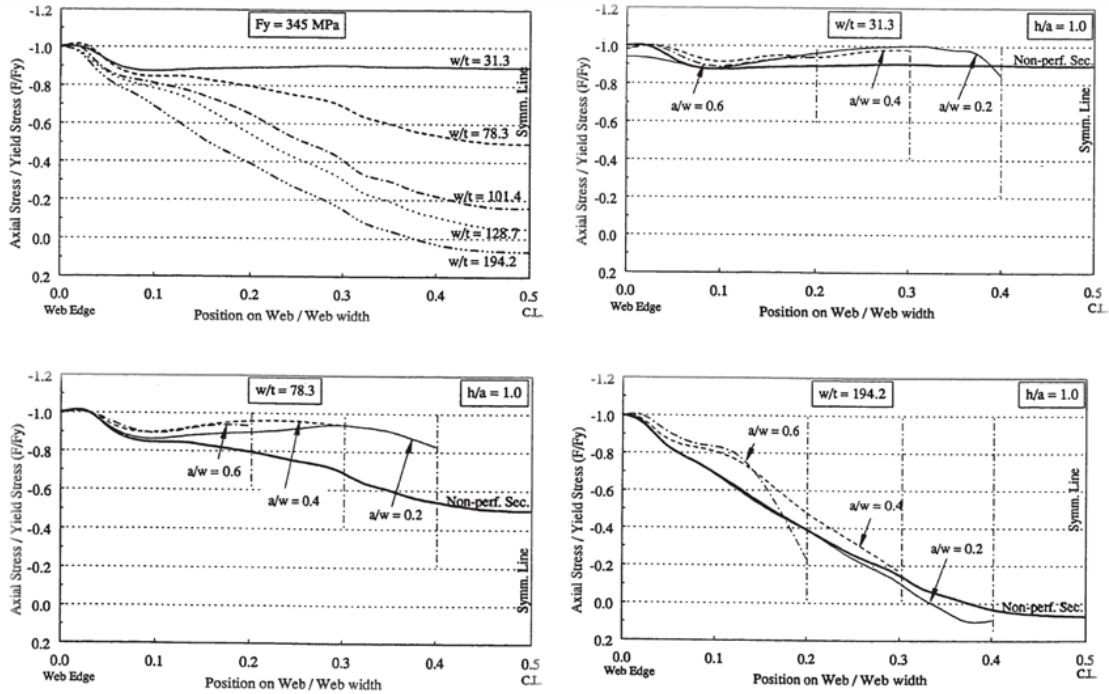


Figure 2.3: Axial stress distributions of non-perforated compression web plates (Abdel-Rahman,1998)

2.3 Steel Section under buckling load

S. Junid (1992) review about the available method to analyse the lateral buckling of tapered I-beams. The method that being used is the Finite Integral Method, the Finite Element Method, the Finite Difference Method and a Power Series Method. In this study, Finite Element method is discussed for flexural-torsional buckling method of analyses. In the finite element method, a tapered member is broken into a number of uniform beam elements with unknown stiffnesses,

which are superimposed to produce the stiffness of the member. A set of displacement is used to describe approximately the deformed state of the structure in terms of the displacement at the nodal points. In Figure 2.4, show the mathematical idealization to form matrix. The energy concept in the conventional analysis of an elastic liner structure is often being used to derive the first-order stiffness matrix of the element. The energy concept is often to derive the first-order stiffness matrix of the element. In order to establish the second order load displacement relationship, the energy concept can be employed in elastic buckling problems. In elastic buckling problems, the conventional linear stiffness matrix is supplemented by another matrix called the geometric matrix. This metric will represent the elastic effect of the applied load on the buckling deformation.

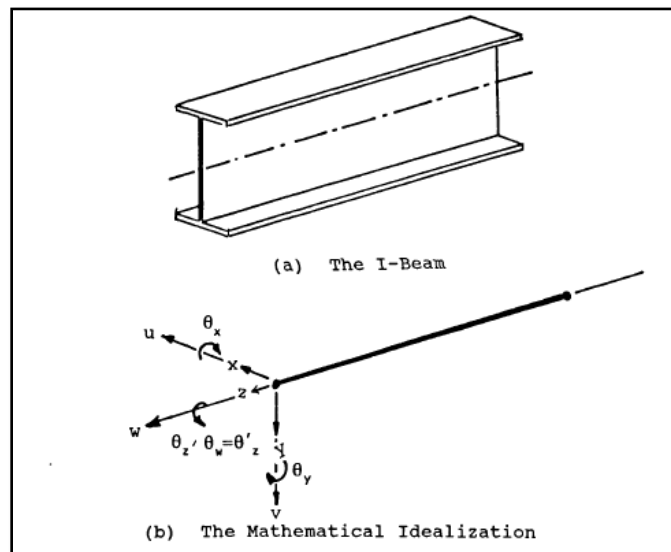


Figure 2.4: The 7 Degree-of-freedom 2-node Beam Element (Mansur, 1992)

Abidin and Izzudin (2013) study local buckling analysis of the steel beam with irregular web opening of various shapes and size. This study is using a castellated beam with 2 original holes of the beam and the regular holes were introduced near to the end support. The presence of

circular holes near the end support cause changes of failure behaviour from buckling of web post (Figure 2.4). The result shows the buckling capacity of modified beam decreasing when holes were created in the end support. In particular, having an opening near to end support is that main factor that leads to the lowest critical buckling load.

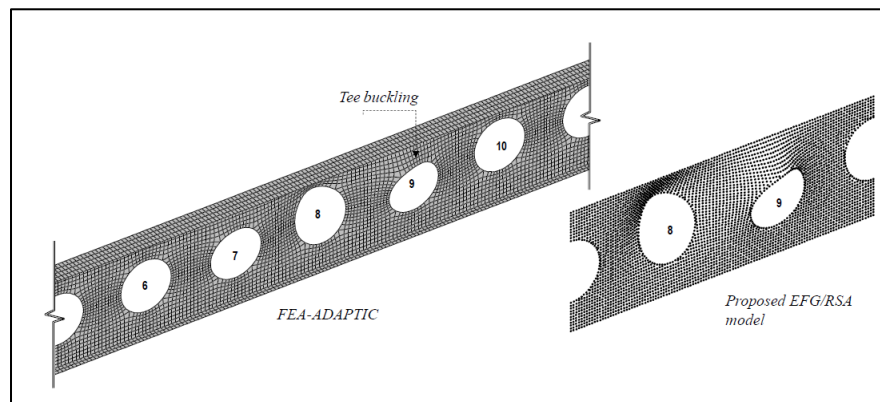


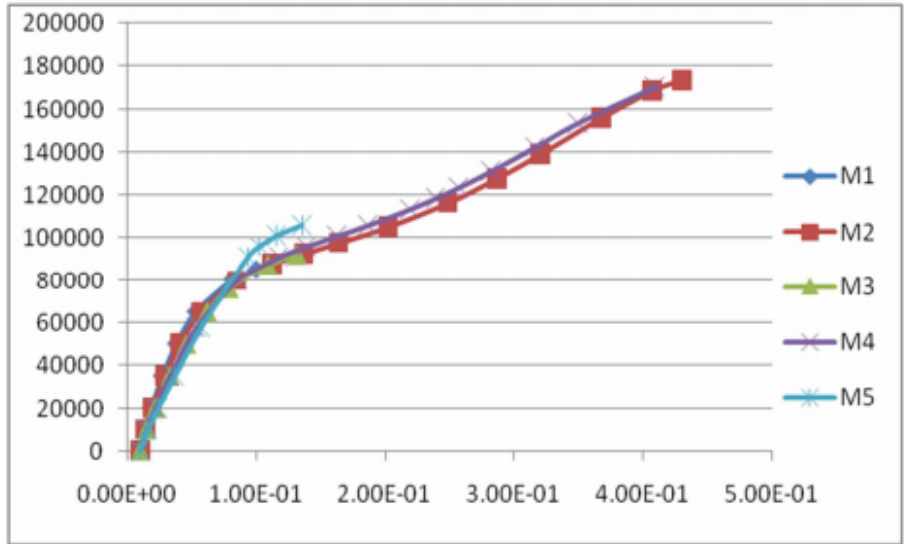
Figure 2.5: Critical buckling modes with FEA-ADAPTIC and EFG/RSA models
(Abidin and Izzudin, 2013)

Furthermore, Using finite element analysis in order to determine the critical inplane longitudinal load at which elastic load buckling of the web of cellular beam- column element occur (Sweeden and Sawy, 2011). The interaction between the flange and the perforate web is approximated by having an aspect ratio ($L/h_w \geq 10$) with multiple circular perforations using finite element modelling. By comparing to the previous study, the different geometrical parameter has effect on the elastic buckling capacity. Azhari et al. (2005) numerical method of virtual work have been used to study local and post-local buckling of stepped and perforated thin plate. When the size parameter increase, the stress distribution become more uniform.

Krishnarani (2016) study about Lateral Torsional Buckling of Corrugated I-beams with Sinusoidal Openings. This study utilising the nonlinear analysis and finite element model to characterise the load-deflection response of castellated I-beam in lateral torsional buckling state. The required three-dimensional finite element model developed by using ANSYS v.16.2, corrugated web. From the Table 2.1, the castellated I beam with the corrugated web at varying corrugation height (h_w) and depth of opening (D_o) with constant S/D_o are considered for each case can withstand maximum load with a minimum rate of deformation. Figure 2.6, Figure 2.7 and Figure 2.8 shows deflection curve under applied load. There are 3 cases involved in this study which have different sizes of the sinusoidal opening (S). At the end of the experiment, the result shows that case 3 has the highest load capacity for every 5 models. From the Table 2.1, it shows that case 3 has the lowest sinusoidal opening compared to case 1 and case 2. So the conclusion of this study, opening in steel section thus affects the steel capacity to resist applied load.

Table 2.1: Parameters consideration for sinusoidal opening (Krishnarani,2016)

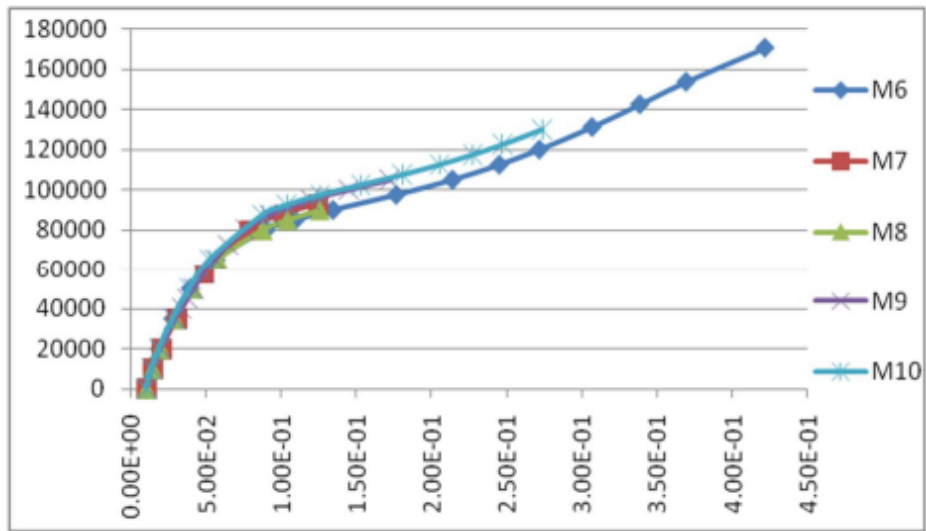
	SI. No	Model	h_w (mm)	D_o (mm)	S (mm)	e (mm)
Case 1	1	M1	700	1.707	574	123
	2	M2	710	1.651	616	132
	3	M3	720	1.531	658	141
	4	M4	730	1.46	700	150
	5	M5	740	1.39	742	159
Case 2	6	M6	700	1.707	533	123
	7	M7	710	1.651	572	132
	8	M8	720	1.531	611	141
	9	M9	730	1.46	650	150
	10	M10	740	1.39	689	159
Case 3	11	M11	700	1.707	492	123
	12	M12	710	1.651	528	132
	13	M13	720	1.531	564	141
	14	M14	730	1.46	600	150
	15	M15	740	1.39	636	159



X axis- Total deformation in m

Y axis- Applied load in N

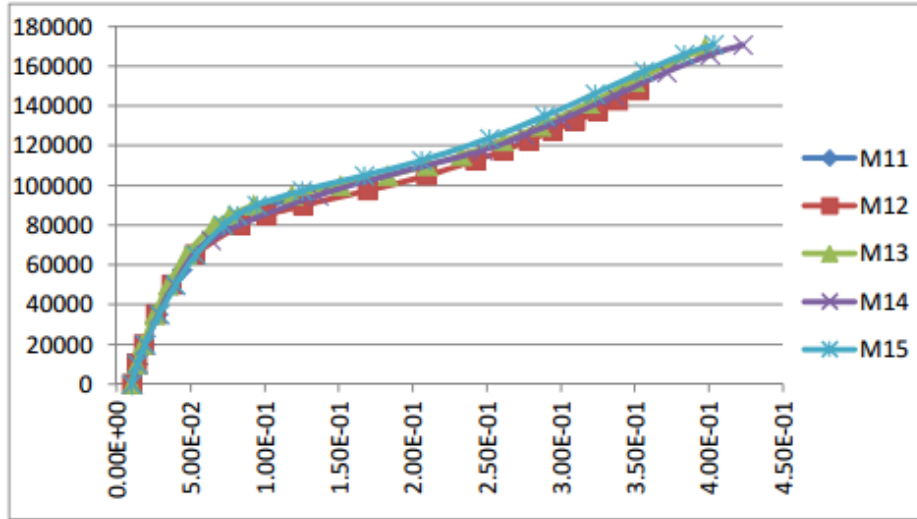
Figure 2.6: Load – Deflection plot for Case 1 FE models (Krishnarani,2016)



X axis- Total deformation in m

Y axis- Applied load in N

Figure 2.7: Load – Deflection plot for Case 2 FE models (Krishnarani,2016)



X axis- Total deformation in m

Y axis- Applied load in N

Figure 2.8: Load – Deflection plot for Case 3 FE models (Krishnarani,2016)

2.4 Cold-formed steel section

Kalavagunta (2013) study about axially compressed cold formed steel channel column. The specimen was tested C-section with axial compression and this section is shown in Figure 2.9. One low voltage displacement transducer was placed at mid of section flange to observe vertical deflection of C-section. Figure 2.8 show Lysaght high tensile C-Lipped channels was selected for the test, yield stresses up to 550 kN/m^2 and is designed in accordance to BS5950-part 5 and AISI specification.



Figure 2.9: Test set up (Kalavagunta, 2013)

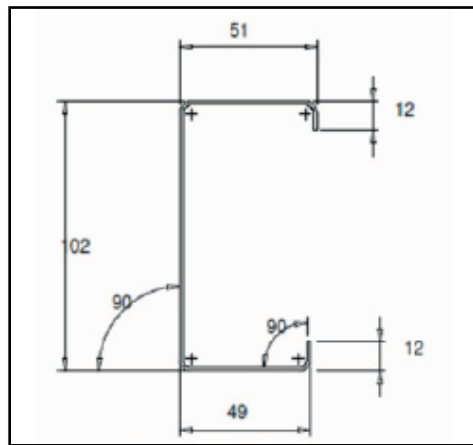


Figure 2.10: Section dimension for C100 section (Kalavagunta, 2013)

The experiment test result of the columns and the theoretical result obtained from BS5950-part 5 and AISI specifications are tabulated (Table 2.2 & Table 2.3). After the comparison of the experiment result and the theoretical value, the experimental test result is very close to DSM and EWM method (Figure 2.11).

Table 2.2: Axial Compression test result Experimental versus
BS5950-Part 5 Theoretical (Kalavagunta, 2013)

Section	F _Y Mpa	Ultimate Axial Compression Capacity- Experiment-kN	Ultimate Axial Compression Capacity- Theoretical-kN
C75 10×500mm	550	57.97	51.98
C75 10×600mm	550	57.88	51.82
C75 10×700mm	550	56.75	51.27
C75 12×500mm	550	72.65	66.75
C75 12×600mm	550	71.08	66.51
C75 12×700mm	550	69.50	65.80
C100 10×500mm	550	68.50	59.98
C100 10×600mm	550	67.90	59.86
C100 10×700mm	550	66.90	59.72

Table 2.3: Axial Compression test result: Experimental versus
AISI Theoretical (Kalavagunta, 2013)

Section	F _Y Mpa	Ultimate Axial Compression Capacity- Experiment-kN	Ultimate Axial Compression Capacity- Theoretical-kN
C75 10×500mm	550	57.97	56.56
C75 10×600mm	550	57.88	55.84
C75 10×700mm	550	56.75	55.00
C75 12×500mm	550	72.65	84.31
C75 12×600mm	550	71.08	83.28
C75 12×700mm	550	69.50	82.08
C100 10×500mm	550	68.50	66.40
C100 10×600mm	550	67.90	66.07
C100 10×700mm	550	66.90	70.08

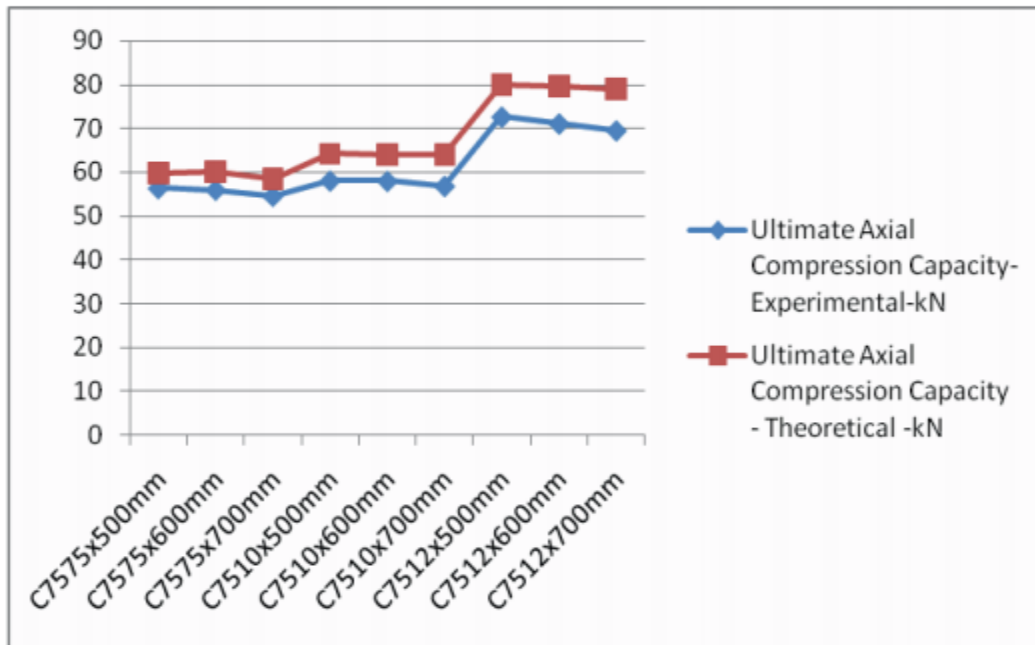


Figure 2.11 Graph Ultimate Load Experimental versus Theoretical (Kalavagunta, 2013)

F. Portioli (2012) study about contact buckling effect in built-up cold-formed steel beams. This study investigates riveted built-up cold-formed patented beam through experiment and numerical analyses. The aim of this study is to compare the effectiveness of the different type of connection system for the beams, including mechanical fasteners and laser welding. Due to web and flange stiffeners and to the configuration of the cross-section, the bending and post-buckling behaviour of the beams is strongly affected by the different source of nonlinearities. Figure 2.12 show two reinforcing plates are placed on the top and bottom hollow flanges of the I-section, providing a flange connection system between the two C-profile. This method can help to prevent early buckling phenomena, intermediate and edge flange stiffeners, web beads and web opening are used.

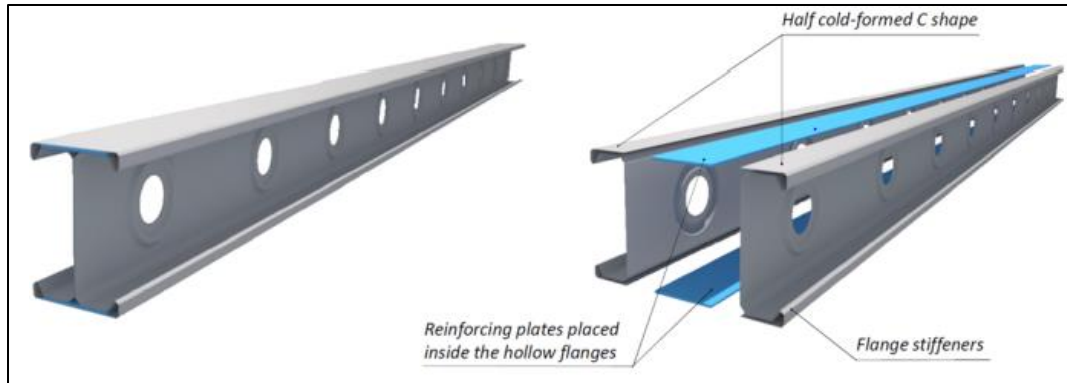


Figure 2.12: MLC Beams (F.Portio,2012)

This experiment performed four-point bending tests. The aim of this investigation is to determine the load bearing capacity of the members. The main geometric details of the MH MLC become are shown in Figure 2.13. The testing program included three prototypes manufactured with different configurations of rivet spacing (d_r) and web stiffeners (f_w) in order to evaluate the effect on the buckling and post-buckling behaviour (Table 2.4).

Table 2.4: Testing program (F.Portio,2012)

Specimen ID	$F_{u,Exp}$	$F_{u,FE}$	$F_{u,Exp}/F_{u,FE}$	$\delta_{u,Exp}$	$\delta_{u,FE}$	$\delta_{e,Exp} / \delta_{u,FE}$
MH MLC 1	112.2	109.2	1.03	38.9	39.5	0.98
MH MLC 2	123.3	124.7	0.99	60.8	59.6	1.02
MH MLC 3	89.40	94.30	0.85	32.6	35.4	0.92

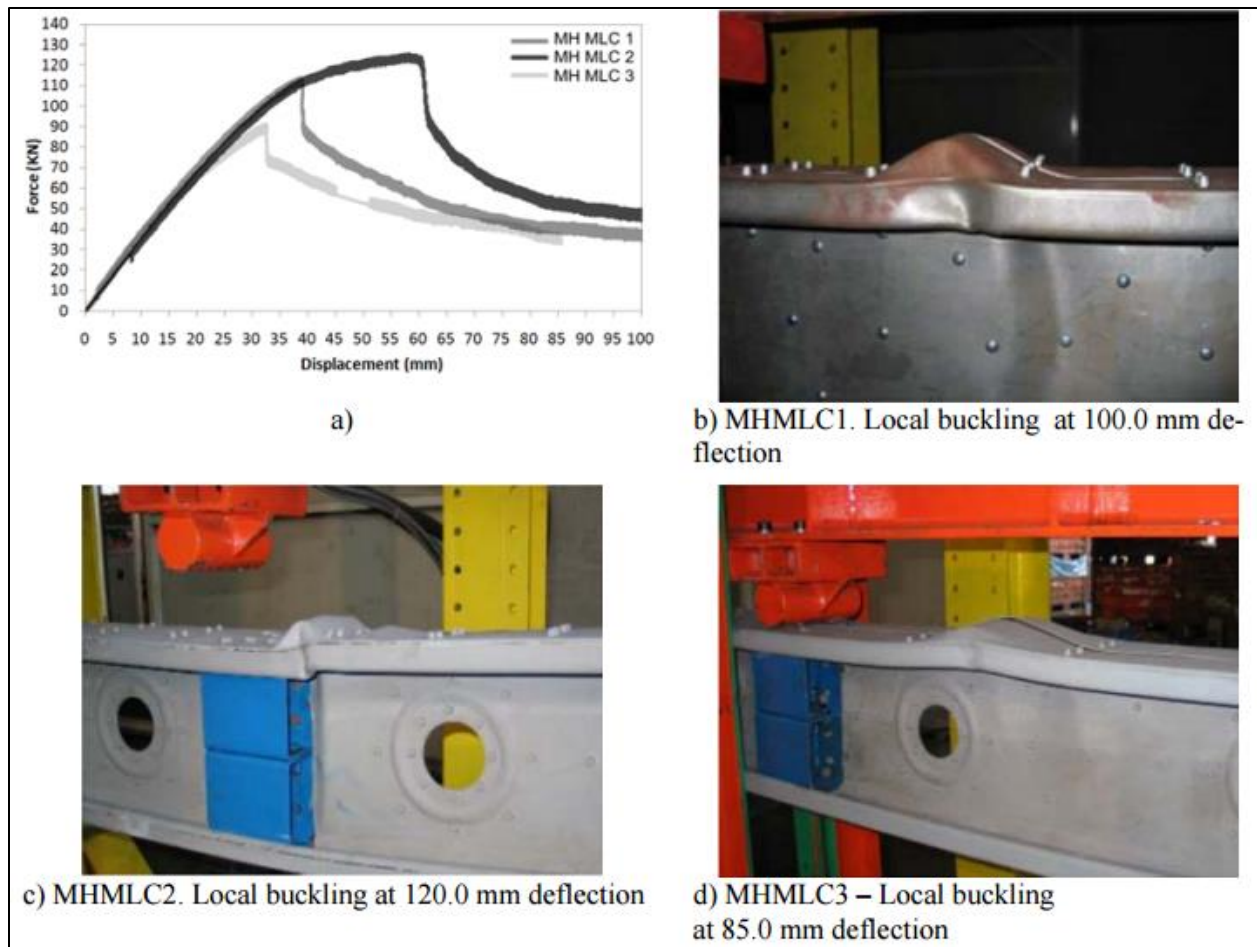


Figure 2.13: Experimental Load Deflection curves of the MLC Beam (F.Portio,2012)

In the experiment, ultimate bending moment M_u have been compared with the yield values M_y , which have been evaluated by considering the gross-section properties. The ratio M_u/M_y is lower than 1.0 for all the tested beams. This shows that the failure modes which have to be ascribed to the buckling load between the fasteners, does not allow all the plastic reserves to be achieved. At the end of the experiment, the force-deflection curve ($F - \delta$) and collapse modes shown in Figure 2.14.

The failure load is slightly influenced by contact force between the cold-formed section and the reinforcing plate in the hollow flange of the beams. Figure 2.12 show the comparison of predicted response curves between with and without contact interaction. In particular, contact effect for spacing of fastener along the flanges which equal to 150mm cause an increment of load bearing capacity up to 11%. More remarkable are influenced by contact interaction on ultimate displacement. The maximum increment obtained from the numerical analysis is about 32% and is calculated for the spacing of 250mm.

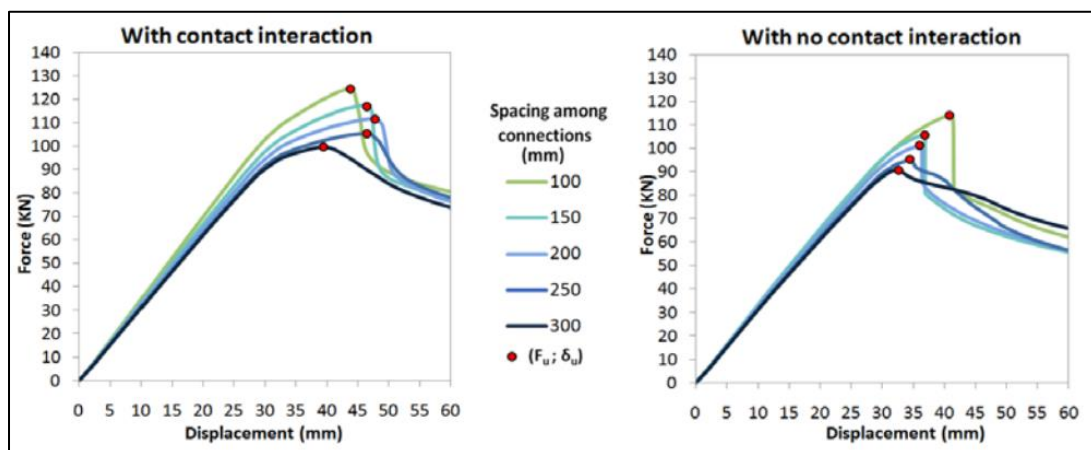


Figure 2.14: Comparison of (F- δ) curve for different connection spacing (F.Portio,2012)

B.P. Gotluru et al., (2000) study about torsion in a thin-walled cold-formed steel beam. Because of the open nature of the sections, torsion induces warping in the beam. This study focuses on a beam which subjected to torque, because the effect of transverse load is not applied at the shear center. This study used CU-BEAM (simple nonlinear analysis) which is a program developed at Cornell University, for the analysis of continuous beams subjected to eccentric transverse load. The stiffness matrix and load vector are derived base on linear finite element analysis.

The results obtained from the analysis were compared with the available experimental result in Gotluru. The rotational behaviour seen in Figure 2.15 indicate that there is some warping fixity in the test. The fixity is considered in the analysis described below. The failure of beam takes place immediately after the yielding on the material. Through the experiment, the yield load predicted by CU-BEAM and the failure load predicted by ABAQUS beam analysis are almost the same. The load-rotation behaviour predicted by both of these methods the same, until yield. The models have illustrated the warping restraint effect in Figure 2.15 the higher the failure load in the case of shell analyses can be attributed to the boundary condition.

In the analysis of all the experiment, it is observed that the beam displaced horizontally and rotates, and no sudden lateral buckling on the beam take place. The result was consistent in this experiment observations (Figure 2.16 & Figure 2.17).

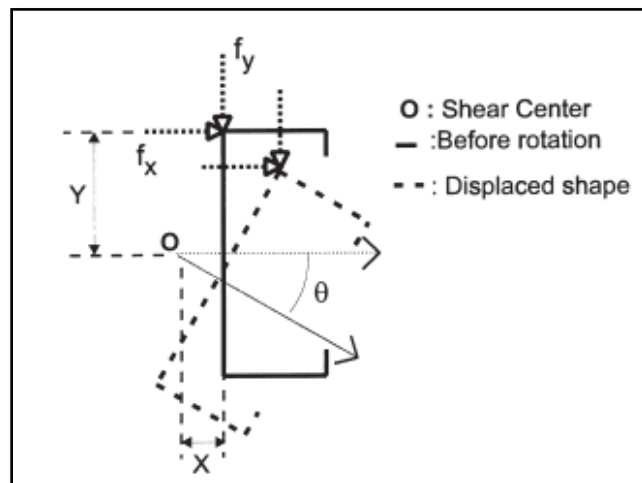


Figure 2.15: CU-BEAM analysis (B.P. Gothuru et al., 2000)

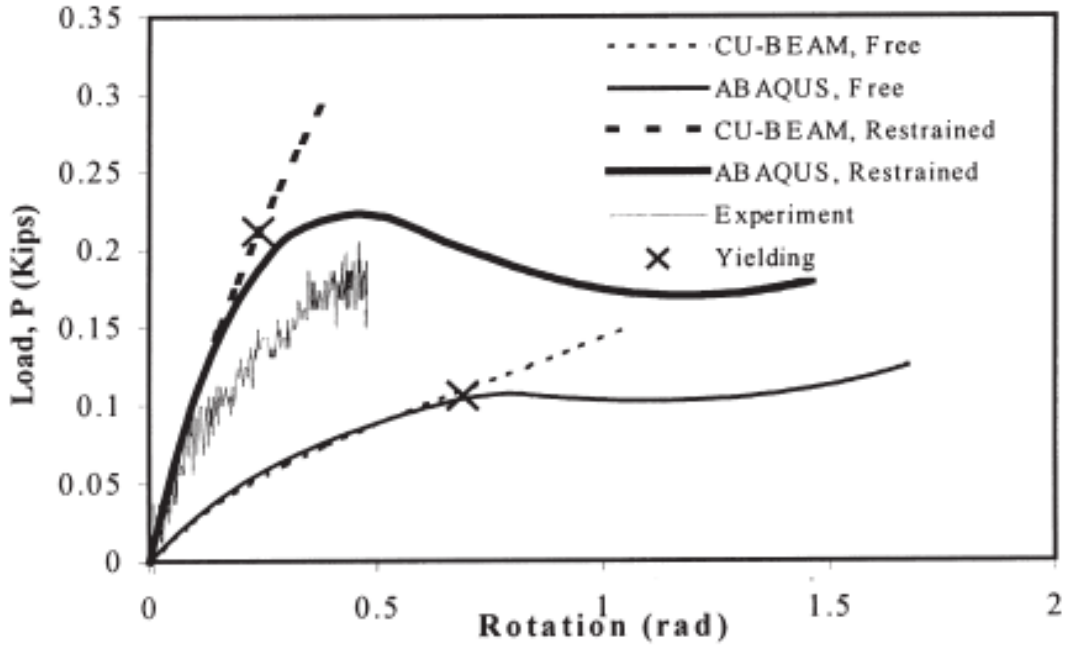


Figure 2.16: Test Rb- Rotation at midspan (B.P. Gothuru et al., 2000)

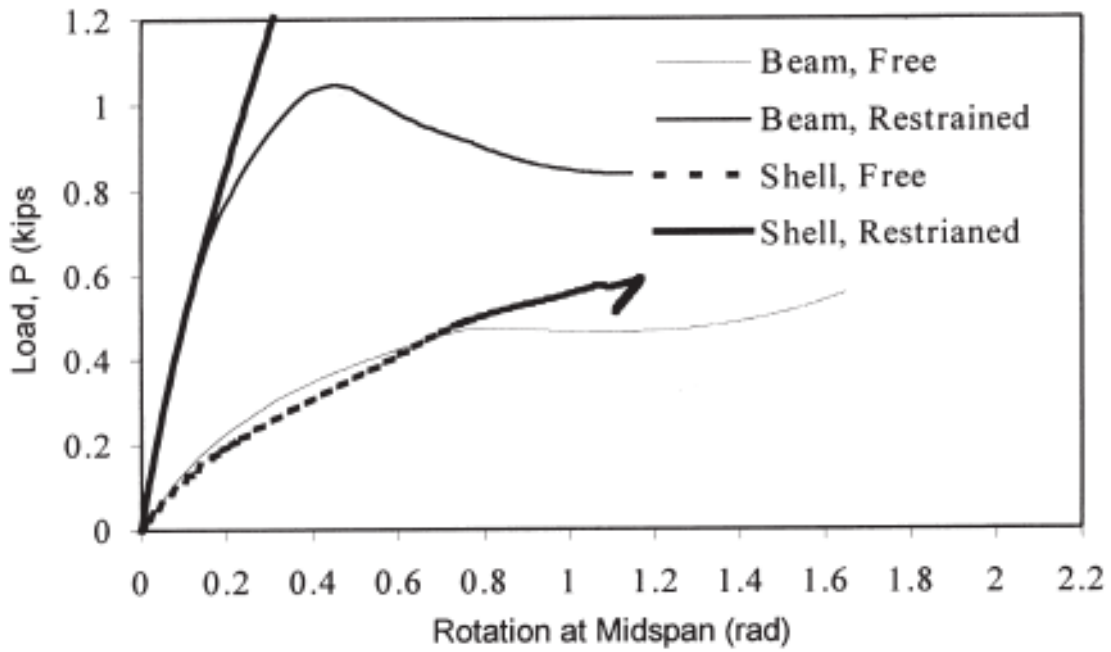


Figure 2.17: Test C12U – effect of warping fixity (B.P.Gothuru,1999)

2.5 Summary

This chapter presents an overall review from the previous researcher on perforated steel. From the literature review, the usage of cold formed C-channel to replace hot rolled steel have many advantages in term of price, strength and steel weight. However, the number of research about cold formed steel with perforation are still limited.

Meanwhile, conclusion for the performance of perforated steel depends on 5 parameters. These parameters include the size of perforation, perforation shape, the spacing between the perforation, number of perforation and the distance between perforation and end of the column. From the discussion in this chapter, found that vierendeel mechanism is the most common mechanism that causes the failure of perforation section. The vierendeel mechanism occurs near the perforation section. Basically, there are several types of perforated shape such as circular, diamond, rectangular, square, and hexagon. The different shape will have different failure mechanism which effects the load capacity of the beam.

In conclusion, cold formed steel with perforation has its own structural performance which needs to discover more. Besides, in the process of designing the best perforation steel member for an affordable house, the strength and structure performance need to study in detail.